GEOPHYSICS. VOL. 76, NO. 5 (SEPTEMBER-OCTOBER 2011); P. WB79–WB86, 13 FIGS.
10.1190/GEO2011-0005.1

Enhanced prestack depth imaging of wide-azimuth data from the Gulf of Mexico: A case history

Xuening Ma[1], Bin Wang[1], Cristina Reta-Tang[1], Wilfred Whiteside[1], and Zhiming Li[1]

ABSTRACT

We present a case study of enhanced imaging of wide-azimuth data from the Gulf of Mexico utilizing recent technologies; and we discuss the resulting improvements in image quality, especially in subsalt areas, relative to previous results. The input seismic data sets are taken from many large-scale wide-azimuth surveys and conventional narrow-azimuth surveys located in the Mississippi Canyon and Atwater Valley areas. In the course of developing the enhanced wide azimuth processing flow, the following three key steps are found to have the most impact on improving subsalt imaging: (1) 3D true azimuth surface-related multiple elimination (SRME) to remove multiple energy, in particular, complex multiples beneath salt; (2) reverse-time migration (RTM) based delayed imaging time (DIT) scans to update the complex subsalt velocity model; and (3) tilted transverse isotropic (TTI) RTM to improve image quality. Our research focuses on the depth imaging aspects of the project, with particular emphasis on the application of the DIT scanning technique. The DIT-scan technique further improves the accuracy of the subsalt velocity model after conventional ray-based subsalt tomography has been performed. We also demonstrate the uplift obtained by acquiring a wide-azimuth data set relative to a standard narrow-azimuth data set, and how orthogonal wide-azimuth is able to enhance the subsalt illumination.

INTRODUCTION

Early forward modeling experiments demonstrated that significant improvements in imaging and multiple attenuation were possible with wide-azimuth data (Regone, 2006; VerWest and Lin, 2007). Initial field data trials quickly followed using ocean-bottom nodes (Ross and Beaudoin, 2006), and streamer data was acquired with a range of acquisition scenarios (e.g., Corcoran et al., 2007; Howard and Moldoveanu, 2006; Threadgold et al., 2006). The results from these surveys confirmed the modeling results and raised interesting questions about how best to optimize the processing sequence for wide-azimuth data (e.g., Michell et al., 2006). As more wide-azimuth data has been acquired, the initial promise of better imaging and reduced multiple content has not consistently been fulfilled. Geophysicists have been working hard to understand the issues involved and to develop processing best practices that result in the maximum amount of uplift from wide-azimuth data (Fromyr et al., 2008).

Our study area is located in Mississippi Canyon and Atwater Valley. The Mississippi Canyon/Atwater Valley area has some of the largest hydrocarbon discoveries in the Gulf of Mexico. Figure 1 shows the TGS wide-azimuth surveys in the area. The Freedom and Liberty wide-azimuth surveys were a cooperative effort between TGS and WesternGeco, and the Justice and Kepler wide-azimuth surveys were acquired and processed by TGS. The Kepler survey is located inside the Justice survey area and was shot in the orthogonal direction relative to the Justice survey, with the goal being to improve subsalt illumination. For comparison, we have a narrow-azimuth data set available in the study area which allows us to study the improvement gained by acquiring wide-azimuth data relative to standard narrow-azimuth data. We also compare the image quality resulting from different anisotropic migration algorithms (Kirchhoff versus reverse-time migration [RTM]) by using the same velocity model and the same wide-azimuth input data.

In our enhanced wide-azimuth processing flow, the following three key steps are found to have the most impact on improving subsalt imaging: (1) 3D true azimuth surface-related multiple elimination (SRME) to remove multiple energy, in particular, complex multiples beneath salt; (2) RTM-based delayed imaging time (DIT) scans to update the complex subsalt velocity model; and (3) tilted transverse isotropic (TTI) RTM to improve the image quality. To obtain a more accurate 3D multiple prediction for wide-azimuth

Manuscript received by the Editor 13 January 2011; revised manuscript received 20 April 2011; published online 22 November 2011.
[1]TGS-NOPEC, Imaging Services, Houston, TX, USA. E-mail: Xuening.Ma@tgsnopec.com; Bin.Wang@tgsnopec.com; Cristina.Reta-Tang@tgsnopec.com; Will.Whiteside@tgsnopec.com; Zhiming.Li@tgsnopec.com.

data, it is important to take the source-to-receiver azimuth into consideration, among other important factors, such as data regularization and interpolation. For refining the sediment velocity model below salt, conventional ray-based tomography was run followed by DIT scans. To improve the overall imaging of this geologically complex area, we see significant uplift by accounting for anisotropy with TTI imaging as compared with vertical transverse isotropic (VTI) imaging from a previous processing project.

In this paper, we first briefly illustrate the effectiveness of true azimuth 3D SRME for removing complex multiples, thereby improving the salt model building process and the resulting subsalt image. We then focus on the application of RTM-based DIT scans for subsalt velocity model building and the image enhancement gained by using TTI RTM over VTI RTM. Finally, we demonstrate the subsalt illumination enhancement that can be obtained by orthogonal wide-azimuth acquisition.

PREDICTING AND REMOVING SUBSALT MULTIPLES

To make 3D SRME more effective for multiple prediction for wide-azimuth data sets, we take into consideration the following two aspects: (1) true source-to-receiver azimuth; and (2) coarse sampling in the crossline direction. For a narrow-azimuth data set, typically the sailing direction is used as the azimuthal direction for the whole data set. However, due to the broad azimuth distribution enabled by a wide-azimuth survey, the single azimuth assumption breaks down. Instead for every trace, we use the true azimuth defined by the source and receiver locations to design the multiple prediction operation (Cai et al., 2009a). In our true azimuth 3D SRME, we perform cable interpolation that resolves the issue of coarse receiver sampling in the crossline direction while retaining the true azimuth information. The details of how cable interpolation improves multiple prediction for wide-azimuth data, especially for complex diffraction multiples, are referred to by Cai et al. (2009b).

Figure 2 shows an example of migrated images with and without true azimuth 3D SRME applied. Without 3D SRME, subsalt primaries are contaminated by strong top of salt and bottom of salt multiples that make subsequent subsalt velocity model updating difficult.

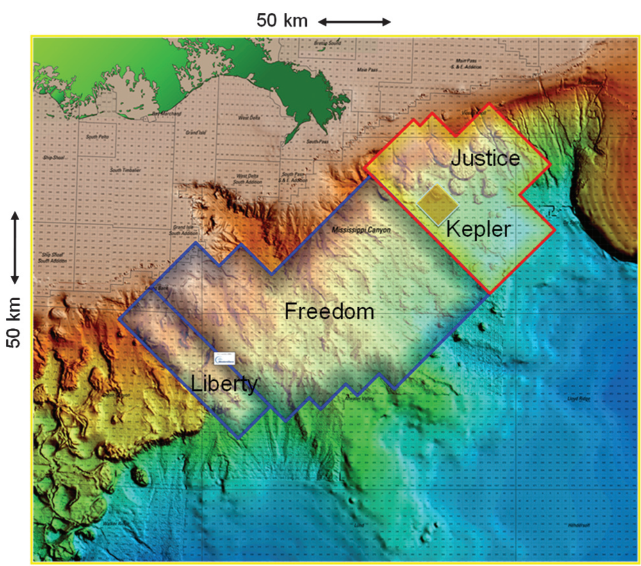

Figure 1. Wide azimuth surveys in the study area.

UPDATING SUBSALT VELOCITY MODEL USING DIT SCANS

RTM-based DIT scans

As a method for updating sediment velocities below salt, subsalt velocity perturbation scans (Wang et al., 2004, 2006a) can be effective, but the cost of generating migration scans is linearly proportional to the number of scans, since multiple passes of migration must be performed, one for each of the scaled velocity models. Constrained by the computation cost and run time, the number of velocity perturbation scans produced is typically limited to between seven to nine scans. To reduce the cost Wang et al. (2005, 2006b, 2009) proposed an alternative subsalt scanning technique by using DIT scans based on focusing analysis (DeVries and Berkhout, 1984; Faye and Jeannot, 1986; M. E. Willis, private communication, 1990; MacKay and Abma, 1992; Audebert and Diet, 1993; Nemeth, 1995, 1996; Wang et al., 1995, 1998, 2005). With DIT scans, a single pass of migration is required, but multiple images can be produced by applying several non-zero-time imaging conditions in addition to the standard zero-time imaging condition (DeVries and Berkhout, 1984; M. E. Willis, private communication, 1990; Wang et al., 1995, 1998, 2005; Sava and Fomel, 2006).

We have developed a new methodology of subsalt velocity updating by using RTM-based DIT scans (Wang et al., 2009), which consists of the following main components: (1) the generation of subsalt RTM-based DIT scans, (2) the picking of DIT values by comparing different RTM-based DIT-scan images, and (3) a subsalt velocity update by using the picked DIT values.

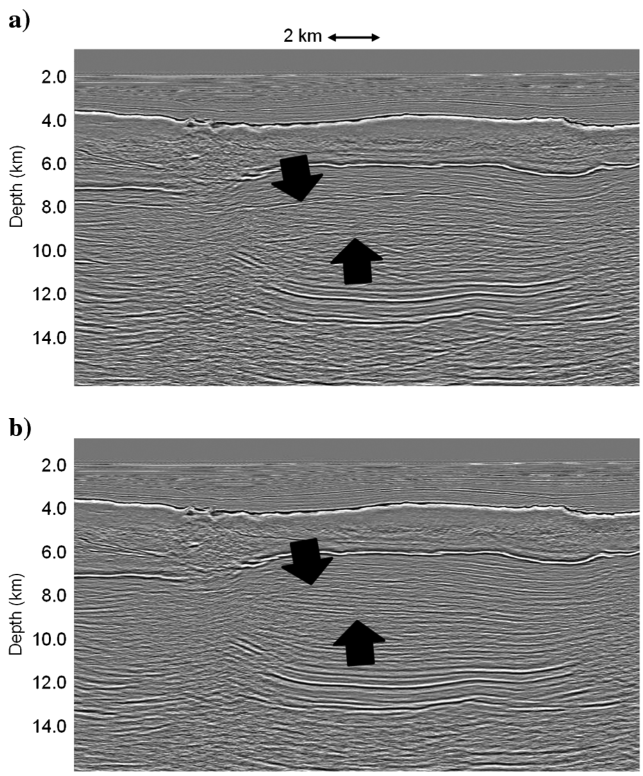

Figure 2. (a) Wide-azimuth prestack depth migration (PSDM) without SRME; (b) wide-azimuth PSDM with 3D SRME.

To be able to generate an RTM-based DIT-scan set, any existing RTM program can be easily modified to apply a zero-time as well as a non-zero-time imaging condition. Once the scan set is prepared, picking of the events can begin. The picking tool for DIT scans is very similar to those originally designed for regular wave-equation migration-based velocity perturbation scan picking (Wang et al., 2006a); but instead of using a velocity scaling factor, the picked value is the time shift (such as −100 ms or +200 ms). Both stacked sections and gathers are used for picking. To facilitate picking accuracy, gathers are also converted to pseudosemblance. Figure 3 shows an example of DIT-scan panels. Clearly, for this example, with the negative time shift, the subsalt events are much better focused.

Composite RTM image-based DIT-scan picking

One benefit of performing DIT-scan analysis is the ability to produce a better focused composite image. To produce the composite image, we first convert each time-shifted DIT-scan image to the pseudodepth domain by applying the following steps: (1) depth-to-time conversion; (2) compensation for the time shift applied during the time-shift imaging condition; and (3) time-to-depth conversion. The composite image can be generated interactively during the picking process to evaluate the validity of the picks.

Figure 4a shows the DIT-value picking interface. Figure 4b shows the regular, zero-time RTM image, and Figure 4c is a real data example of the composite image after the DIT-scan picking by using the Freedom wide-azimuth data set. Compared to the regular RTM image (Figure 4b), the composite image (Figure 4c) is much better focused and subsalt events are more coherent. This indicates that the trend of the updated picks is correct.

The composite image can be used for two purposes: (1) to QC the DIT-scan picking; and (2) to produce the best focused final image. The composite image must be equal or better in quality as compared to the regular image corresponding to DIT equal to zero. Any degradation of the composite image in any part of the image indicates picking errors. The composite image (Figure 4c) based on the DIT-scan picking is better focused and more coherent as compared to the regular RTM image (Figure 4b).

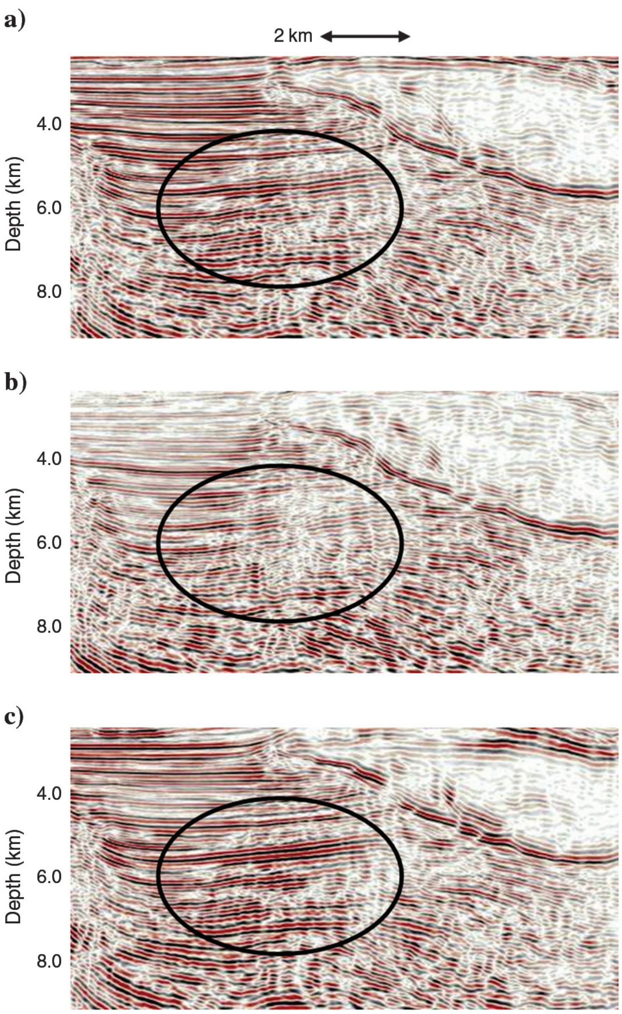

Figure 3. An example of DIT-scan panels with delayed imaging times: (a) 0 ms; (b) +100 ms; (c) −100 ms.

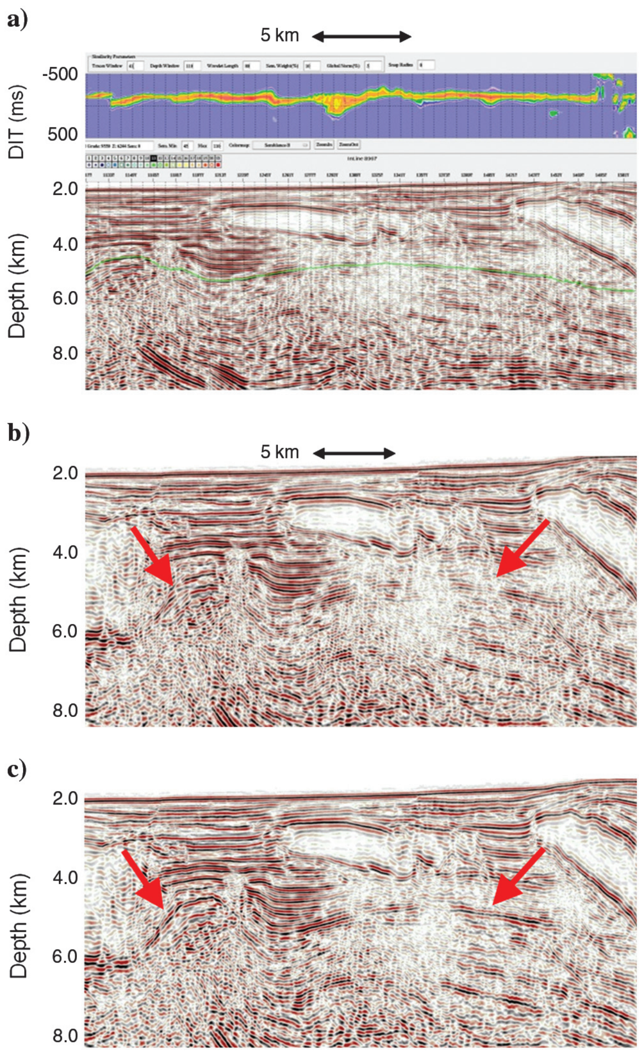

Figure 4. a) DIT-scan picking interface; (b) Regular RTM image using initial velocity model; (c) Composite RTM image using the same initial velocity model after DIT scans.

Subsalt velocity update by using RTM-based DIT scans

The RTM-based DIT-scan subsalt velocity update methodology has been successfully applied to a few proprietary and multiclient wide-azimuth processing projects to update the subsalt velocity models.

Figure 5 shows an inline example of the RTM images from the Freedom wide-azimuth survey before and after the subsalt velocity update using the RTM-based DIT-scan method. For this example, 21 RTM-based DIT-scan images are produced. The initial velocity model already has ray-based subsalt tomography, which is well-suited for most of the subsalt velocity model. By using our subsalt scan picking tool, delayed imaging times are picked by comparing scan panels (stacked images) as well as gather displays. This method is similar to wave-equation migration scan picking (Wang et al., 2008). After the DIT-scan subsalt velocity update, RTM is rerun by using the newly updated velocity model.

By using the new velocity model with the subsalt velocity update using DIT scans, the subsalt RTM image quality is much improved with better focused and more coherent subsalt events.

Figure 6 shows an example crossline display comparing the RTM images before and after the DIT subsalt velocity update. In the highlighted target area, after the DIT scans, the RTM image is much more interpretable, and our interpreters believe the new structure makes more geological sense.

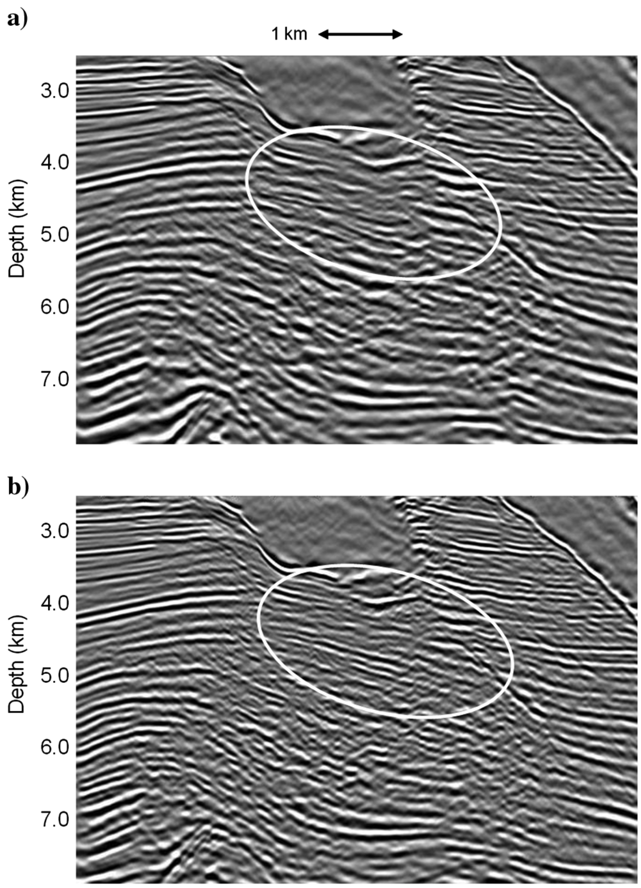

Figure 5. Freedom wide-azimuth RTM images: (a) Using initial subsalt velocity model; (b) Using velocity model updated with subsalt DIT scans.

RTM FOR SALT MODEL BUILDING AND SUBSALT IMAGING

RTM for salt model building

Due to its superior image quality, RTM is used for producing final migration images, and for velocity model creation, especially for salt model building. Compared to other migration algorithms, such as Kirchhoff and one-way wave-equation migration, RTM has the following strengths: (1) like Kirchhoff migration, RTM is capable of imaging steep-dip events, therefore it is good for producing images of steeply dipping salt flanks and salt overhangs; (2) like wave-equation migration, RTM is not ray-based but is a direct implementation of the wave equation; therefore it is accurate in handling sharp velocity contrasts such as across salt boundaries, and it has multipathing capability which is one key for imaging complex areas such as subsalt; and (3) RTM is based on the two-way wave equation; therefore, it is able to handle other complex wave modes, such as diving waves and multiple-bounce prism waves, which one-way wave-equation migration is not able to handle. In some shallow areas right below steep-dip base of salt, prism waves may add some additional angle illumination and improve the image quality.

Figure 7 is an example showing the image comparison between TTI Kirchhoff and TTI RTM by using the same inputs and same model. TTI RTM is able to image the complex salt overhang much better than TTI Kirchhoff. Clearly, RTM is the best algorithm for complex salt model building.

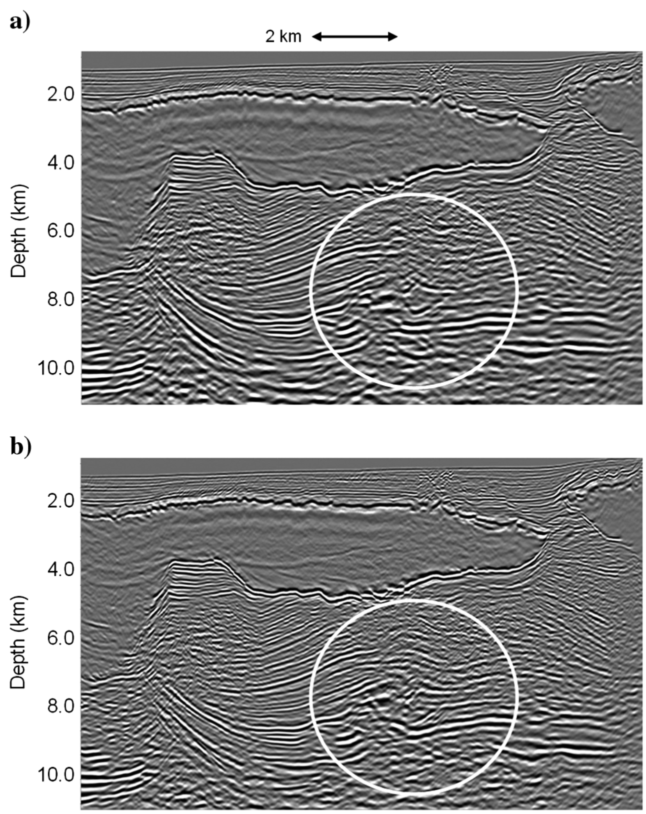

Figure 6. Freedom wide azimuth (a) RTM image before DIT scans; (b) RTM image after DIT scans.

TTI RTM image enhancement

In parts of the study area, the geologic structures are very complex with dipping sediments and complex salt intrusions. Previously, we performed VTI RTM imaging with the same input data. For most areas with relatively simple geological structure, VTI was very suitable as VTI RTM yielded a good image. However, in some areas with complex structure, we needed a TTI model to more accurately capture the complexity.

Figure 8 shows one example of how TTI RTM is able to improve the image quality compared to VTI RTM. Figure 8a is the final image from the previous imaging product by using VTI RTM, and Figure 8b is the most recent imaging product using TTI RTM. TTI RTM significantly enhanced subsalt image focusing and coherency, and improved the accuracy of event positioning, especially in the highlighted shadow area right below the bottom of salt. Our geologists believe that maintaining the dipping trend toward the bottom of salt in the TTI RTM image makes more geological sense as compared to the curved down structure near the bottom of salt in the VTI RTM image. Though the cost of running TTI RTM is about three times the cost of running VTI RTM, the uplift in TTI RTM image quality can justify the cost. As a result, TTI RTM is rapidly becoming the industry standard for Gulf of Mexico depth imaging projects, especially where there is well control.

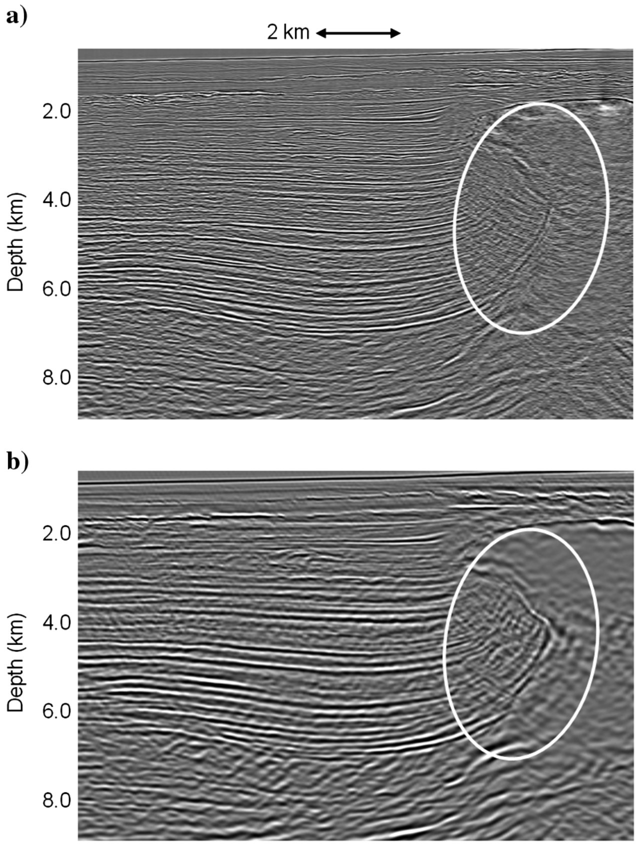

Figure 7. Example for imaging complex salt overhang: (a) TTI Kirchhoff migration image; (b) TTI RTM image.

SUBSALT ILLUMINATION ENHANCEMENT WITH ORTHOGONAL WIDE AZIMUTH

Subsalt illumination enhancement with wide-azimuth acquisition

In addition to creating a more accurate velocity model using TTI RTM and subsalt DIT scans, image improvements were also obtained due to better illumination. Before the wide-azimuth data was acquired in the study area (Figure 1), we acquired a large multiclient narrow-azimuth survey called Mississippi Canyon Revival (Figure 9) roughly overlapping the new wide-azimuth surveys. It is well-known that with the additional acquisition aperture in the crossline direction, subsalt illumination can be much improved with a wide-azimuth survey as compared to a narrow-azimuth survey.

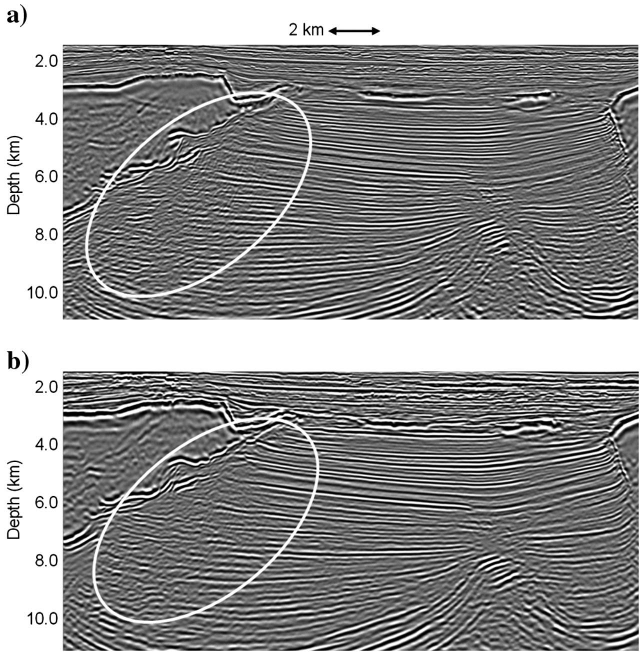

Figure 8. Example in the shadow area right below steeply dipping bottom of salt: (a) VTI RTM image; (b) TTI RTM image.

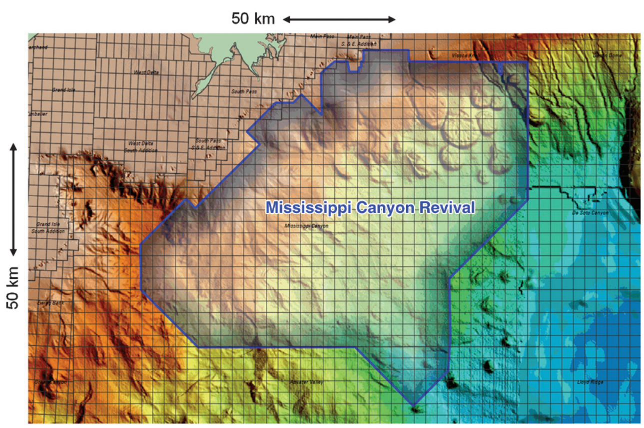

Figure 9. Mississippi Canyon Revival narrow-azimuth survey (approximately 660 blocks).

In Figures 10 and 11, we show a few examples of image comparisons between a narrow-azimuth survey and a wide-azimuth survey.

Figure 10 shows an image comparison in the inline direction between the Mississippi Canyon Revival narrow-azimuth survey and the Freedom wide-azimuth survey. Figure 10a shows an example inline display of the final VTI Kirchhoff image from the narrow-azimuth Mississippi Canyon Revival project. Figure 10b shows the final VTI Kirchhoff image from Freedom wide-azimuth of the same line, and Figure 10c is the corresponding final VTI RTM image from Freedom wide-azimuth. Some of the wide-azimuth image quality enhancement is due to the improved model building enabled by additional azimuthal information, but both the narrow-azimuth and wide-azimuth products are our best-effort results. The great uplift seen in the wide-azimuth final images can be largely attributed to the enhancement of increased subsalt illumination. Comparing Figure 10c to Figure 10b, we can see the additional value of RTM imaging versus Kirchhoff imaging, since the same model was used for both migrations. RTM improved the subsalt image quality and showed a much better sediment event termination toward the salt boundary, especially in the shallow areas right below the steep-dip bottom of salt, as illustrated around the salt body on the right-hand side.

As shown in Figure 1, our Justice wide-azimuth survey is the northeast extension of the Freedom wide-azimuth survey. Justice wide-azimuth was acquired in 2010, and data processing and imaging are still ongoing. A part of the Justice wide-azimuth survey also overlaps our previous Mississippi Canyon Revival narrow-azimuth survey.

Figure 11 shows image comparisons of the Mississippi Canyon Revival narrow-azimuth survey to the Justice wide-azimuth survey. Though images of the Justice wide-azimuth data set are just fast-track results, they clearly demonstrate superior image quality as compared to the Mississippi Canyon Revival final images. The wide-azimuth acquisition of Justice significantly improved overall image quality as compared to the narrow-azimuth Mississippi Canyon Revival data set. The RTM image has additional uplift, especially in the subsalt areas, due to its multipathing capability and accuracy of modeling wave-propagation through complex areas with sharp velocity contrasts.

Illumination enhancement with orthogonal wide-azimuth acquisition

One of the goals that wide-azimuth acquisitions aim to achieve is to extend the crossline offset and azimuthal coverage. The question might be asked, how wide in the crossline direction is considered wide enough? Like a typical wide-azimuth survey, our Justice wide-azimuth survey has a maximum crossline offset of approximately 4 km on each side of the sail line. To more effectively increase the crossline offset and improve the overall azimuthal coverage, an overlapping wide-azimuth survey called Kepler wide-azimuth

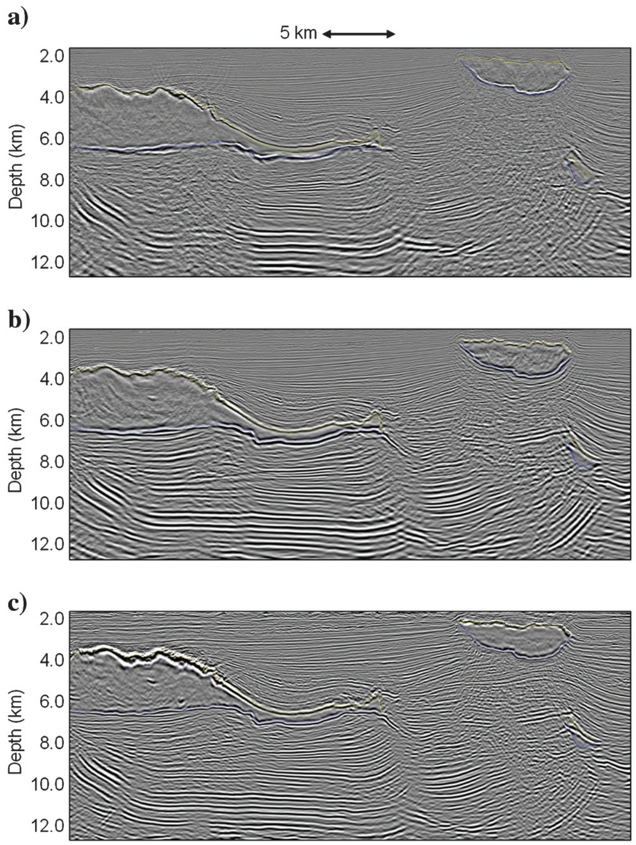

Figure 10. Example inline image: (a) Mississippi Canyon Revival narrow-azimuth VTI Kirchhoff; (b) Freedom wide-azimuth VTI Kirchhoff; (c) Freedom wide-azimuth VTI RTM.

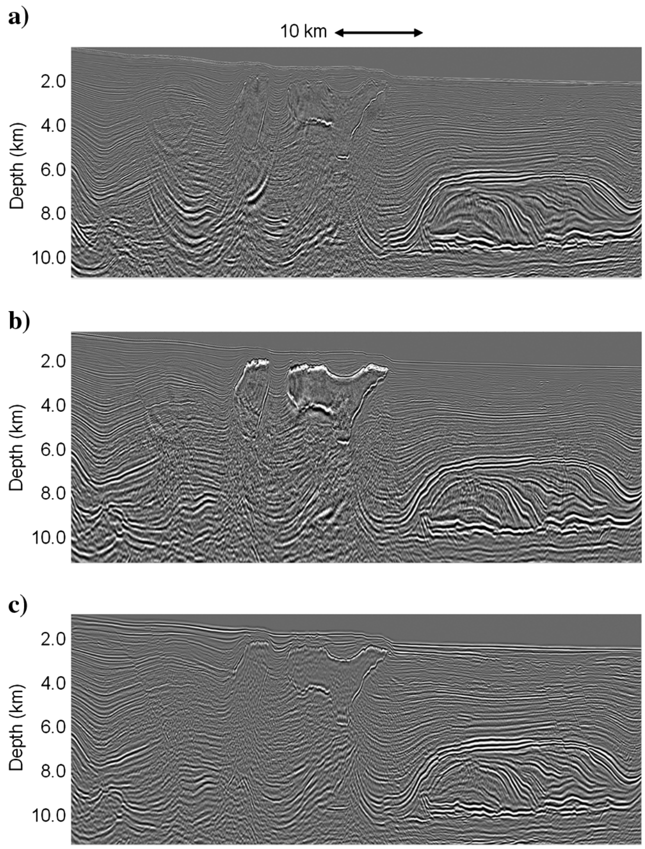

Figure 11. Example inline image: (a) Mississippi Canyon Revival narrow-azimuth VTI Kirchhoff; (b) fast-track Justice wide-azimuth VTI Kirchhoff; (c) fast-track Justice wide-azimuth VTI RTM.

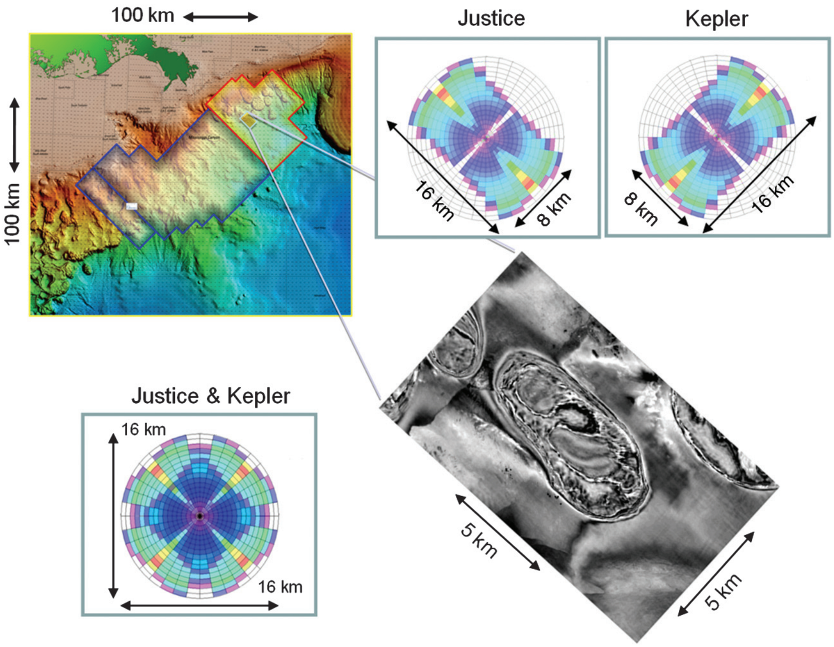

Figure 12. Orthogonal wide-azimuth surveys: Justice and Kepler.

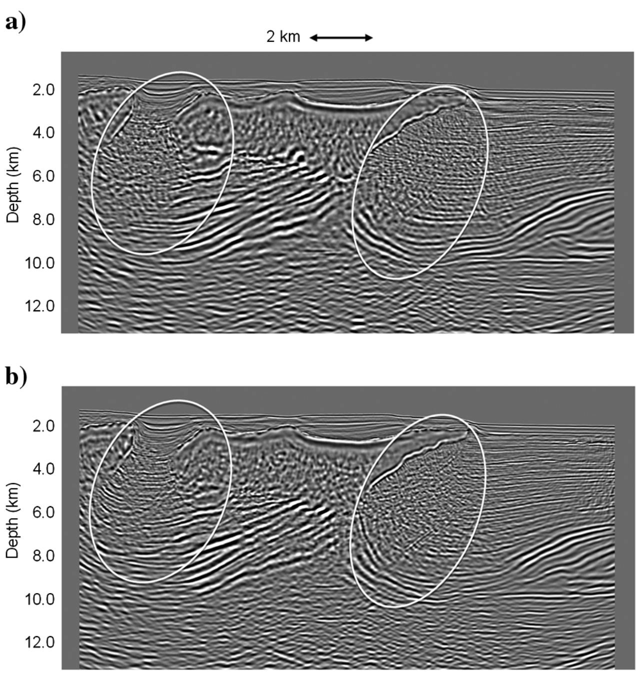

Figure 13. Comparison of Justice and Kepler RTM images: (a) fast-track RTM inline example of Justice wide-azimuth survey; (b) fast-track RTM crossline example of Kepler wide-azimuth survey.

was shot inside the Justice survey area, with the sailing direction orthogonal to the Justice survey.

Figure 12 illustrates the orientation of the two orthogonal wide-azimuth surveys. As shown by the azimuth-offset rose diagrams, the Justice survey was shot in the northwest-southeast direction, while the Kepler survey was shot in the northeast-southwest direction. Although each wide-azimuth survey has significant crossline offset and extended azimuthal coverage, clearly the combination of the two orthogonal wide-azimuth surveys achieves much more uniform azimuthal coverage as illustrated by the rose diagram in the lower left corner.

Due to the mutual orthogonality of the two surveys, inlines from Justice are parallel to crosslines from Kepler. Figure 13a is an example inline RTM image from the Justice survey, and Figure 13b is the overlying crossline RTM image from the Kepler survey. On the right-hand side of Figure 13a, we can see that the Justice survey provides much better illumination in the shadow area right below the bottom of salt. However, on the left-hand side of Figure 13b, Kepler shows more coherent sediment reflections in the minibasin area between the two salt bodies, and Kepler also images the subsalt events better in the middle of the figure. The images from the two surveys complement each other.

CONCLUSION

We have described several processing technologies that have resulted in significant improvements in the seismic imaging results for a few current projects. We have illustrated that true azimuth 3D SRME is an effective approach to remove complex subsalt multiples. Additionally, a new methodology using RTM-based delayed imaging time scans has been developed and successfully applied to a few wide-azimuth processing projects. The DIT subsalt scanning method is an efficient replacement for the more conventional subsalt velocity perturbation scans. We demonstrated that DIT subsalt scans provide additional improvement to subsalt velocity models after application of the more conventional ray-based subsalt tomography step.

We also showed benefits of using RTM over other migration algorithms. RTM combines the strength of Kirchhoff steep-dip imaging and the multipathing capability of the one-way wave-equation migration. Additionally, RTM has the ability to handle two-way wave-propagation modes, such as diving waves and prism waves. Due to its ability to handle complex velocity models and produce superior image quality, TTI RTM has become a routine tool in building salt models as well as producing final migration images. We also demonstrated substantial improvement in the subsalt image quality with wide-azimuth data as compared to the results from a previous narrow-azimuth survey. The newly acquired orthogonal wide-azimuth surveys illustrate the benefit of illumination enhancement due to their expanded azimuthal coverage.

ACKNOWLEDGMENTS

We would like to thank many of our TGS colleagues for their contributions to this paper. We thank our processing team, particularly the following people for producing the figures used in this paper: Gary Rodriguez, George Cloudy, Zhiqiang Guo, Amy Liu, and Ashley Lundy. We also thank many in our R&D group for producing the tools used in production: James Cai, Sang Suh, Kwangjin Yoon, Jean Ji, Alex Yeh, Manhong Guo, and Sampath Gajawada. Additional thanks to Laurie Geiger, Chuck Mason, and Simon Baldock for reviewing and proofreading the paper. Finally, we thank TGS management for permission to publish this paper and WesternGeco management for permission to show the Freedom data.

REFERENCES

Audebert, F., and J. P. Diet, 1993, Migrated focus panels: Focusing analysis reconciled with prestack depth migration: 62nd Annual International Meeting, SEG, Expanded Abstracts, **12**, 961–964, doi: 10.1190/1.1822668.

Cai, J., S. Dong, M. Guo, S. Sen, J. Ji, B. Wang, and Z. Li, 2009b, Some aspects on data interpolation: Multiple prediction and imaging: 79th Annual International Meeting, SEG, Expanded Abstracts, **28**, 3178–3181, doi: 10.1190/1.3255517.

Cai, J., M. Guo, S. Sen, S. Dong, R. Camp, and B. Wang, 2009a, From SRME or wave-equation extrapolation to SRME and wave-equation extrapolation: Annual International Meeting, SEG, Expanded Abstracts, **28**, 3313–3316, doi: 10.1190/1.3255507.

Corcoran, C., C. Perkins, D. Lee, P. Cattermole, R. Cook, and N. Moldoveanu, 2007, A wide-azimuth streamer acquisition pilot project in the Gulf of Mexico: The Leading Edge, **26**, 460, doi: 10.1190/1.2723210.

DeVries, D., and A. J. Berkhout, 1984, Influence of velocity errors on the focusing aspects of migration: Geophysical Prospecting, **32**, 629–648, doi: 10.1111/gpr.1984.32.issue-4.

Faye, J. P., and J. P. Jeannot, 1986, Prestack migration velocities from focusing depth analysis: 56th Annual International Meeting, SEG, Expanded Abstracts, 438–440.

Fromyr, E., P. Wijnen, R. van Borselen, P. Aaron, and L. Comeaux, 2008, An exploration-scale wide azimuth towed streamer case study: 78th Annual International Meeting, SEG, Expanded Abstracts, **27**, 1008–1012, doi: 10.1190/1.3059098.

Howard, M. S., and N. Moldoveanu, 2006, Marine survey design for rich-azimuth seismic using surface streamers: 76th Annual International Meeting, SEG, Expanded Abstracts, **25**, 2915, doi: 10.1190/1.2370132.

MacKay, S., and R. Abma, 1992, Imaging and velocity estimation with depth focusing analysis: Geophysics, **57**, 1608–1622, doi: 10.1190/1.1443228.

Michell, S., E. Shoshitaishvili, D. Chergotis, J. Sharp, and J. Etgen, 2006, Wide azimuth streamer imaging of Mad Dog; Have we solved the subsalt imaging problem?: 76th Annual International Meeting, SEG, Expanded Abstracts, **25**, 2905, doi: 10.1190/1.2370130.

Nemeth, T., 1995, Velocity estimation using tomographic depth-focusing analysis: 65th Annual International Meeting, SEG, Expanded Abstracts, **14**, 465–468, doi: 10.1190/1.1887351.

Nemeth, T., 1996, Relating depth-focusing analysis to migration velocity analysis: 66th Annual International Meeting, SEG, Expanded Abstracts, **15**, 463–466, doi: 10.1190/1.1826675.

Regone, C., 2006, A modeling approach to wide-azimuth design for subsalt imaging: The Leading Edge, **25**, 1467, doi: 10.1190/1.2405331.

Ross, A., and G. Beaudoin, 2006, Field design and operation of a deep water, wide azimuth node seismic survey: 76th Annual International Meeting, SEG, Expanded Abstracts, **25**, 2920–2924, doi: 10.1190/1.2370133.

Sava, P., and S. Fomel, 2006, Time-shift imaging condition in seismic migration: Geophysics, **71**, no. 6, S209–S217, doi: 10.1190/1.2338824.

Threadgold, I. M., K. Zembeck-England, P. Gunnar Aas, P. M. Fontana, D. Hite, and W. E. Boone, 2006, Implementing a wide azimuth towed streamer field trial: The what, why and mostly how of WATS in Southern Green Canyon: 76th International Annual Meeting, SEG, Expanded Abstracts, **25**, 2901–2904, doi: 10.1190/1.2370129.

VerWest, B., and D. Lin, 2007, Modeling the impact of wide-azimuth acquisition on subsalt imaging: Geophysics, **72**, no. 5, SM241, doi: 10.1190/1.2736516.

Wang, B., V. Dirks, P. Guillaume, F. Audebert, and D. Epili, 2006a, A 3D subsalt tomography based on wave-equation migration-perturbation scans: Geophysics, **71**, no. 2, E1–E6, doi: 10.1190/1.2187720.

Wang, B., V. Dirks, P. Guillaume, F. Audebert, A. Hou, and D. Epili, 2004, 3D sub-salt tomography based on wave equation migration perturbation scans: 74th Annual International Meeting, SEG, Expanded Abstracts, **23**, 2375–2378, doi: 10.1190/1.1839699.

Wang, B., Y. Kim, C. Mason, and X. Zeng, 2008, Advances in velocity model-building technology for subsalt imaging: Geophysics, **73**, no. 5, VE173–VE181, doi: 10.1190/1.2966096.

Wang, B., C. Mason, M. Guo, K. Yoon, J. Cai, J. Ji, and Z. Li, 2009, Subsalt velocity update and composite imaging using reverse-time-migration based delayed-imaging-time scan: Geophysics, **74**, no. 6, WCA159–WCA167, doi: 10.1190/1.3227152.

Wang, B., and K. Pann, 1998, Model-based interpretation of focusing panels for depth focusing analysis: 68th Annual International Meeting, SEG, Expanded Abstracts, **17**, 1596–1599, doi: 10.1190/1.1820224.

Wang, B., K. Pann, and J. E. Malloy, 1995, Macro velocity model estimation through model-based globally-optimized depth focusing analysis: 57th Annual International Conference and Exhibition, EAGE, Extended Abstracts, session E038.

Wang, B., F. Qin, V. Dirks, P. Guillaume, F. Audebert, and D. Epili, 2005, 3D finite angle tomography based on focusing analysis: 78th Annual International Meeting, SEG, Expanded Abstracts, **24**, 2546–2549, doi: 10.1190/1.2148242.

Wang, B., D. Wheaton, F. Audebert, and V. Dirks, 2006b, Separation of focusing and positioning effects using wave equation based focusing analysis and post-stack modeling: 76th Annual International Meeting, SEG, Expanded Abstracts, **25**, 2646–2649, doi: 10.1190/1.2370132.